Available online at www.sciencedirect.com
SCIENCE DIRECT®
Journal of Molecular Catalysis A: Chemical 211 (2004) 73–81
JOURNAL OF MOLECULAR CATALYSIS A: CHEMICAL
www.elsevier.com/locate/molcata

Enantioselective hydrogenation of tiglic acid in methanol and in dense carbon dioxide catalyzed by a ruthenium–BINAP complex substituted with OCF_3 groups

Xing Dong, Can Erkey*

Department of Chemical Engineering, Environmental Engineering Program, University of Connecticut, 191 Auditorium Road, Storrs, CT 06269, USA

Received 7 August 2003; received in revised form 14 October 2003; accepted 14 October 2003

Abstract

A fluorinated analog of the 2,2′-bis(diphenylphosphino)-1,1′-binaphthyl (BINAP) ligand was synthesized with OCF_3-substitution of the aryl groups in BINAP skeleton (*p*-OCF_3–BINAP). Ruthenium complexes of both BINAP (Ru–BINAP) and (*p*-OCF_3)–BINAP (Ru–[(*p*-OCF_3)–BINAP]) were also synthesized and investigated as catalysts for hydrogenation of tiglic acid in methanol. Typically, Ru–[(*p*-OCF_3)–BINAP] had lower activity but had higher enantioselectivity at high hydrogen pressures than Ru–BINAP at the same condition. The effect of OCF_3 groups on the catalytic properties was discussed on the basis of NMR spectra and kinetic data. Ru–[(*p*-OCF_3)–BINAP] was found to have sufficiently high solubility in dense CO_2 for homogeneous catalytic reactions and was investigated for hydrogenation of tiglic acid in CO_2. The results showed that CO_2 had a great influence on both activity and enantioselectivity. Addition of methanol to CO_2 was found to increase the enantioselectivity.

Keywords: BINAP; Fluorinated ligands; Tiglic acid; Hydrogenation; Supercritical CO_2

1. Introduction

Chiral chemistry is a rapidly growing field since chiral compounds play a key role in many fields such as agriculture, biology, materials science and life sciences. For example, the worldwide sales for chiral drugs are growing at an annual rate of 13%, and the sales are expected to reach US$ 200 billion in 2008 [1]. Over the past several decades, catalysis by chiral organometallic complexes has emerged as one of the most attractive approaches in the production of chiral chemicals. This method can multiply chirality with a catalytic amount of chiral source contained in the catalysts.

Despite its advantages and efficiency, industrial applications of chiral catalysis are limited partly due to the difficulties associated with recovery and recycle of the expensive catalysts from reaction mixtures. Therefore, novel reaction media for organometallic chemistry, which include supercritical fluids (SCFs) [2], ionic liquids [3], fluorous liquids [4] and liquid biphasic systems [5] are being investigated for chiral catalysis. For example, Pozzi et al. [6] reported the first chiral fluorous biphasic catalysis in 1998 by using C_2 nitrogen-based ligands. Subsequently, several promising results with different fluorous catalysts were described [7–9]. Francio et al. [10] showed that by using rhodium complexes of the perfluoroalkyl-substituted ligand, (*R*,*S*)-3-H^2F^6–BINAPHOS, a large variety of substrates could be hydroformylated in $scCO_2$ with rates and enantioselectivities comparable to those obtained in a benzene solution with the conventional catalyst.

An important issue that needs to be addressed in development of fluorinated complexes is the effect of highly electron withdrawing property of fluorous groups on catalytic activity and selectivity. A few studies have been reported in the literature on this effect for fluorinated catalysts. It was found that the activity of fluorinated rhodium complexes in the hydroformylation of olefins in $scCO_2$ increased with decreasing basicity of phosphines [11,12]. Further investigation by in-situ FTIR spectroscopy showed that this enhancement was due to a shift in the equilibrium distribution of the catalytically active intermediates [13]. On the other

* Corresponding author. Tel.: +1-860-486-4601; fax: +1-860-486-2959.
E-mail address: cerkey@engr.uconn.edu (C. Erkey).

1381-1169/$ – see front matter © 2003 Published by Elsevier B.V.
doi:10.1016/j.molcata.2003.10.016

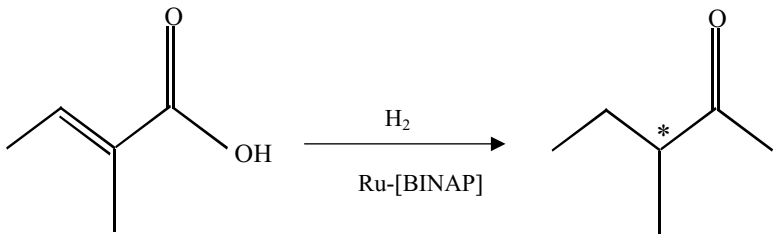

Scheme 1. Tiglic acid hydrogenation reaction.

hand, Horvath et al. [14] found that arylphosphine ligands gave more reactive rhodium catalysts than alkylphosphine ligands, and the fluorine substituents in the ligands further retarded the reaction rate in the hydroboration of norbornene in the fluorous solvent $CF_3C_6H_5$. These studies indicate that there is a need to study the influence of the fluorous groups on activity and enantioselectivity of chiral organometallic catalysts for a wide variety of reactions.

The ruthenium complexes containing 2,2′-bis(diphenylphosphino)-1,1′–binaphthyl (BINAP) are the most extensively used catalysts in many enantioselective reactions [15]. Among those, the enantioselective hydrogenation of unsaturated acids such as tiglic acid (Scheme 1) is of significant interest because of the unique efficacy of the Ru–BINAP complexes in these reactions and the high economic value of the products, which afford useful building blocks for the synthesis of non-steroidal anti-inflammatory agents [16]. In this article, we report the synthesis of a fluorinated BINAP ligand and its ruthenium complex, as well as our results on the hydrogenation of tiglic acid in methanol and in dense CO_2 catalyzed by this new complex and the conventional ruthenium–BINAP complex.

2. Experimental section

2.1. General methods for preparation of Ru–BINAP and Ru–[(p-OCF_3)–BINAP] complexes

All phosphine compound syntheses were carried out under a nitrogen atmosphere. (*R*)-(−)-1,1′-Bi-2-naphthol bis (trifluoro methanesulfonate), 1-bromo-4-(triflouromethoxy) benzene, diethyl phosphite, trichlorosilane, triethyl amine were purchased from Aldrich and magnesium turnings were obtained from Acros. All the chemicals were used as received. The synthetic scheme for fluorinated BINAP and Ru–BINAP type complexes is shown in Scheme 2.

2.2. Synthesis of **1b**

1-bromo-4-(triflouromethoxy)benzene (25 g, 0.104 mol) was added slowly with stirring to magnesium turnings (2.74 g, 0.115 mol) and ether (25 ml), and heated under reflux for 30 min. To the cooled reagent, diethyl phosphite (7 ml, 0.052 mol) in ether (5 ml) was added slowly with stirring, and the whole heated under reflux for 60 min. The mixture was cooled under ice bath and 10% hydrochloric acid (48 ml) was added slowly. The ether layer was extracted with 2% hydrochloric acid (200 ml), and the whole was dried by Na_2SO_4 and evaporated, giving yellowish bis (4-triflouromethoxy)benzene phosphine oxide(13.9 g, 79%). The spectral properties of the product are as follows: ^{1}H NMR (400 MHz, $CDCl_3$) δ: 8.48 ppm (d, 1H, $^1J_{H,P}$ = 495.8 Hz), 8.08 ppm (dd, 4H, $^3J_{H,H}$ = 8.4 Hz, $^3J_{H,P}$ = 13.2 Hz), 7.63 ppm (d, 4H, $^3J_{H,H}$ = 7.8 Hz). ^{31}P NMR (162 MHz, $CDCl_3$) δ: 20.43 ppm (s, decoupled).

2.3. Synthesis of **2b**

Trichlorosilane (2.7 ml) was added slowly with stirring to **1b** (to 2.25 g, 6.64 mmol), triethyl amine (3.84 ml) and toluene (30 ml) under ice bath, and heated under reflux for 4 h. After cooling, 2N sodium hydroxide solution (133 ml) was added slowly under ice bath. The organic layer was combined with ether and evaporated under vacuum, giving the yellow liquid (1.86 g, 87%). The spectral properties of 2 are as follows: ^{1}H NMR (400 MHz, $CDCl_3$) δ: 7.53 ppm (dd, 4H, $^3J_{H,H}$ = 6.8 Hz, $^3J_{H,P}$ = 6.6 Hz), 7.24 ppm (d, 4H, $^3J_{H,H}$ = 7.6 Hz), 5.30 ppm (d, 1H, $^1J_{H,P}$ = 219.7 Hz). ^{31}P NMR (162 MHz, $CDCl_3$) δ: −41.67 ppm (s, decoupled).

2.4. Synthesis of **3b**

To a solution of $NiCl_2$dppe (355 mg) in DMF (10 ml) at room temperature was added **2b** (2.5 g, 7.74 mmol). The solution was heated to 110 °C and kept at this temperature for 30 min. (*R*)-(−)-1,1′-Bi-2-naphthol bis (trifluoro methanesulfonate) (3.6 g, 6.55 mmol) and DABCO (2.9 g) in DMF (20 ml) was added slowly to the above solution. Three additional equal portions of **2b** were added after 1, 3 and 7 h. The reaction was kept at 110 °C until (*R*)-(−)-1,1′-Bi-2-naphthol bis (trifluoro methanesulfonate) was completely consumed (3 days). **3b** (3.2 g, 43%) was obtained by recrystallizion from a mixture of methanol and DMF. The spectral properties of **3b** are as follows: ^{1}H NMR (400 MHz, $CDCl_3$) δ: 7.98 ppm (d, 2H, J = 8.3 Hz), 7.89 ppm (d, 2H, J = 8.0 Hz, $^3J_{H,P}$ = 13.2 Hz), 7.43 ppm (m, 4H), 7.15 ppm (m, 4H), 7.07 ppm (m, 8H), 6.97 ppm (m, 6H), 6.75 ppm (d, 2H, J = 8.8 Hz). ^{31}P NMR (162 MHz, $CDCl_3$) δ: −14.89 ppm (s, decoupled). Elemental analysis: $C_{48}H_{28}F_{12}O_4P_2$ requires C: 60.12%; H: 2.93%; F: 23.80%, found C: 59.87%; H: 2.49%; F: 24.80%.

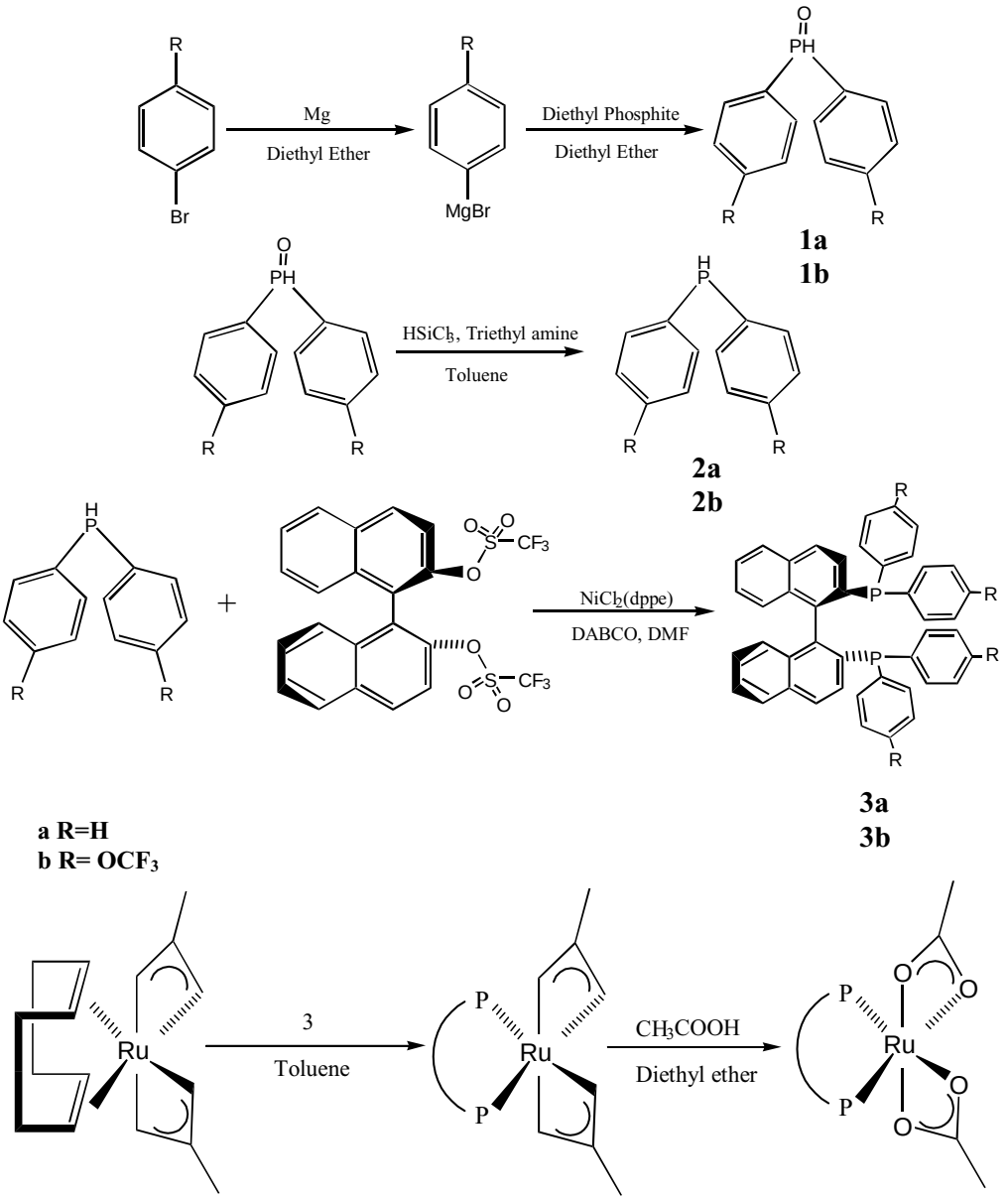

Scheme 2. Synthetic procedure for BINAP and (p-OCF_3)–BINAP and their complexes with ruthenium.

2.5. Synthesis of Ru–BINAP type complexes

A solution of (COD)Ru(methylallyl)$_2$ (168 mg, 0.527 mmol) and **3b** (501 mg, 0.523 mmol) or **3a** (325 mg, 0.523 mmol) in toluene (20 ml) was heated under reflux for 4 h and the toluene was evaporated under vacuum. A solution of acetic acid (2 ml) in ether (15 ml) was added at room temperature and the resulting solution was stirred for 10–14 h. Ru–BINAP complexes (402 mg, 91%) and Ru–[(p-OCF_3)–BINAP] (527 mg, 86%) were obtained as yellow-brown solid. The spectral properties of Ru–BINAP are as follows: ^{1}H NMR (400 MHz, $CDCl_3$) δ: 7.84 ppm (m, 4H), 7.45 ppm (m, 12H), 7.21 ppm (t, 2H, J = 7.2 Hz), 7.09 ppm (m, 4H), 6.89 ppm (t, 2H, J = 8.4 Hz), 6.63 ppm (d, 2H, J = 8.7 Hz), 6.50 ppm (m, 6H). ^{31}P NMR (162 MHz, $CDCl_3$) δ: 65.06 ppm (s, decoupled). The spectral properties of Ru–[(p-OCF_3)–BINAP] are as follows: ^{1}H NMR (400 MHz, $CDCl_3$) δ: 7.84 ppm (m, 4H), 7.55 ppm (t, 4H, J = 8.9 Hz), 7.32 ppm (m, 8H), 7.14 ppm (m, 4H), 7.00 ppm (t, 2H, J = 8.4 Hz), 6.67 ppm (d, 2H, J = 8.4 Hz), 6.18 ppm (d, 4H, J = 10.8 Hz). ^{31}P NMR (162 MHz, $CDCl_3$) δ: 64.88 ppm (s, decoupled).

2.6. General procedure for investigation of the tiglic acid hydrogenation reactions

The experimental set-up is shown in Fig. 1. The reactor is a custom manufactured, 54 ml stainless steel vessel fitted with two sapphire windows (1 in. i.d., Sapphire Engineering), polyether–ether–ketone o-rings (Valco Instruments),

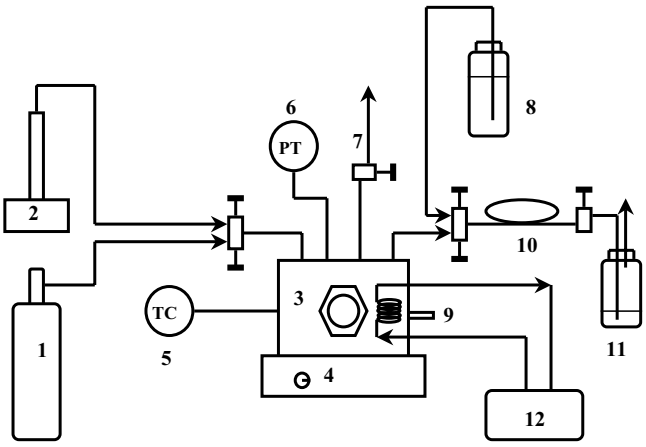

Fig. 1. Experimental set-up. (1) Hydrogen cylinder, (2) syringe pump, (3) windowed reactor, (4) stir plate, (5) thermocouple assembly, (6) pressure transducer, (7) vent line, (8) solvent reservoir, (9) rupture disk assembly, (10) sample loop, and (11) sample collection vial.

a T-type thermocouple assembly (Omega Engineering, DP41-TC-MDSS), a pressure transducer (Omega Engineering, PX300-7.5KGV), a vent line, and a rupture disk assembly (Autoclave Engineers). When methanol was used as a solvent, a certain amount of tiglic acid and catalyst was placed into the reactor. Then the reactor was sealed and the air was removed by flushing with nitrogen several times. A certain amount of degassed methanol was charged into the reactor, and the vessel was heated to the desired temperature. The reaction was started by charging the reactor with hydrogen. When CO_2 was used as a solvent, the procedure was the same as above except that the catalyst was isolated in an ampoule, and the air was removed by flushing with hydrogen several times. Subsequently, a certain amount of hydrogen was charged, followed by charging with CO_2 using a high-pressure syringe pump (ISCO 260D). During this period, the ampoule broke and the reaction started.

The samples were taken periodically using the sampling system shown in Fig. 1. The valve between high-pressure sample loop and the reactor was opened periodically to take samples. The sample was then depressurized into a sample vial. Subsequently, the sample loop was flushed with a small amount of acetone from a reservoir. The sample loop was further dried with compressed air. The collected samples were analyzed by gas chromatography (HP 6890) equipped with a CP-Chiralsil-DEX CB column.

3. Results

The effect of hydrogen pressure on reaction rate for hydrogenation of tiglic acid in methanol was investigated in the pressure range of 3.4 ∼ 95.3 bar and 3.4 ∼ 25.2 bar with fluorinated and conventional Ru–BINAP complexes, respectively. In all cases, the catalyst concentration was kept constant as 0.3 mM. The data are given in Figs. 2 and 3 indicate that the rate increases with increasing hydrogen pressure.

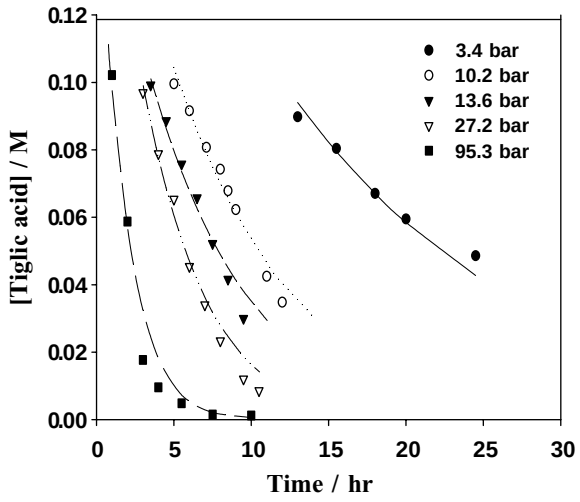

Fig. 2. Hydrogen pressure effect on the tiglic acid hydrogenation reactions in methanol catalyzed by [(*p*-OCF_3)–BINAP]Ru[O_2CCH_3]$_2$ {[tiglic acid]$_0$ = 0.125 M, [catalyst] = 0.3 mM, T = 25 °C}.

The results also show that the reaction rate with Ru–BINAP was much higher than that with Ru–[(*p*-OCF_3)–BINAP] at the same hydrogen pressure. The hydrogen pressure effect on enantioselectivity is given in Fig. 4 and shows that the enantioselectivity did not change with pressure for hydrogen pressures less than 13.6 bar. However, the enantioselectivity decreased with further-increasing hydrogen pressure.

The effect of the tiglic acid concentration on reaction rate was also investigated in methanol in the range of 1.2 ∼ 500 mM. In all cases, the catalyst concentration was kept constant as 0.3 mM. The data are listed in Figs. 5 and 6 and show that the reaction rate increased with increasing tiglic acid concentration. As shown in Table 1, the initial tiglic acid concentration had no appreciable effect on enantioselectivity.

The rate expression was developed on the basis of above kinetic data. The experimental reaction rate at each data

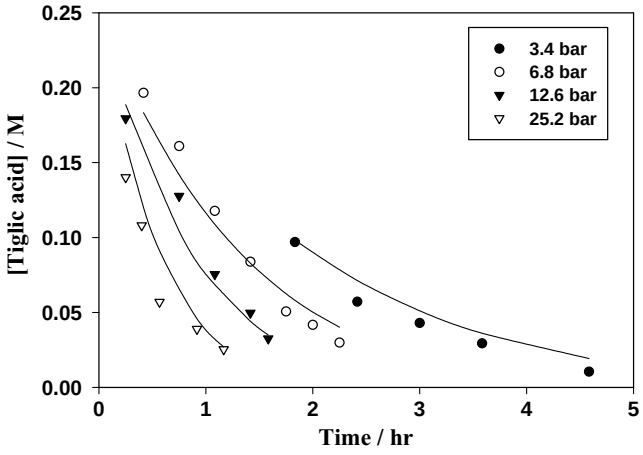

Fig. 3. Hydrogen pressure effect on the tiglic acid hydrogenation reactions in methanol catalyzed by [BINAP]Ru[O_2CCH_3]$_2$ {[tiglic acid]$_0$ = 0.25 M, [catalyst] = 0.3 mM, T = 25 °C}.

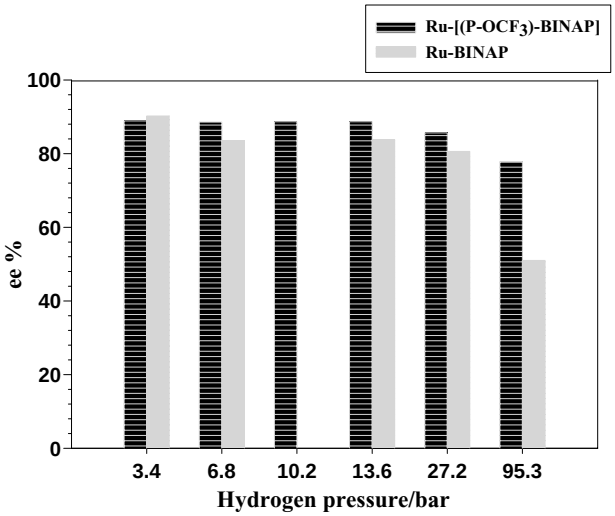

Fig. 4. Hydrogen pressure effect on the enantioselectivity {[tiglic acid]$_0$ = 0.125 M, [catalyst] = 0.3 mM, T = 25 °C}.

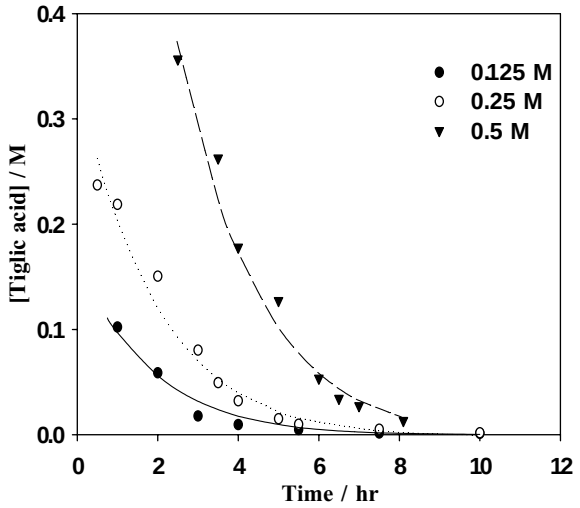

Fig. 5. Tiglic acid concentration effect on the tiglic acid hydrogenation reactions in methanol catalyzed by [(p-OCF$_3$)–BINAP]Ru[O$_2$CCH$_3$]$_2$ {H$_2$ = 95.3 bar, [catalyst] = 0.3 mM, T = 25 °C}.

point was calculated by differentiating the concentration of tiglic acid versus time curves. These experimental reaction rate data together with the experimental concentration data (the concentration of hydrogen at each data point was calculated from the solubility of hydrogen in methanol [17] and the reaction stoichiometry) were used to determine the rate expression by using the Polymath software. The rate expression for the reactions catalyzed by Ru–BINAP in methanol was:

$$-r = 5.672 \times C_a^{0.881} C_b^{0.599}$$

where the rate is given in units of mol dm^{-3} h^{-1} and the concentrations are expressed in mol dm^{-3}. C_a represents the concentration of tiglic acid and C_b represents the concentration of hydrogen. Similar kinetic features were also observed with Ru–[(p-OCF$_3$)–BINAP] complex and the rate expression was found to be:

$$-r = 0.875 \times C_a^{0.929} C_b^{0.627}$$

The degree of fit for the rate expressions is illustrated in Figs. 2, 3, 5 and 6 where the solid curves represent the predicted values that were calculated using the rate expression and the dots represent the experimental data.The reaction was also studied at different temperatures. The experimental data are provided in Figs. 7 and 8. The data were used to determine the activation energy of the reaction from the slope of the plot of ln k versus 1/T. The calculated activation

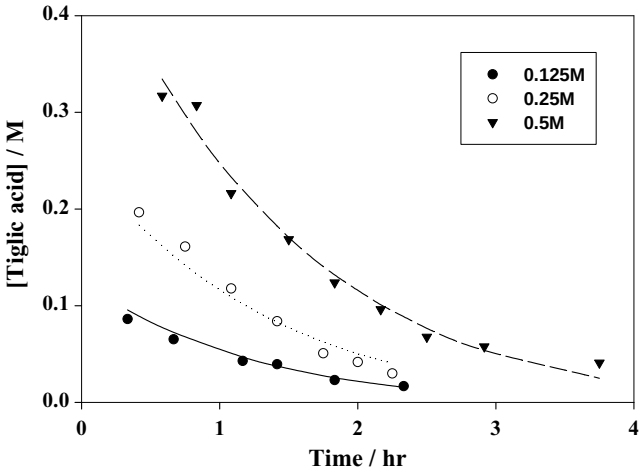

Fig. 6. Tiglic acid concentration effect on the tiglic acid hydrogenation reactions in methanol [BINAP]Ru[O$_2$CCH$_3$]$_2$ {H$_2$ = 95.3 bar, [catalyst] = 0.3 mM, T = 25 °C}.

Table 1
[Tiglic acid]$_0$ and temperature effect on enantioselectivity in methanol

Catalyst	ee (%)									
	Temperature (°C)							[Tiglic acid]$_0$ (M)		
	0	8.6	10.5	22.3	23.5	35.1	36.2	0.125	0.250	0.500
Ru–BINAP	–	82.9[a]	–	–	83.8[a]	84.0[a]	–	83.8[c]	83.1[c]	84.5[c]
Ru–[(p-OCF$_3$)–BINAP]	76.0[b]	–	75.3[b]	77.8[b]	–	–	75.5[b]	77.8[d]	78.6[d]	80.0[d]

[a] H$_2$ = 13.8 bar, catalyst = 0.3 mM, [tiglic acid]$_0$ = 0.25 M.
[b] H$_2$ = 96.5 bar, catalyst = 0.3 mM, [tiglic acid]$_0$ = 0.125 M.
[c] H$_2$ = 13.8 bar, catalyst = 0.3 mM, T = 25 °C.
[d] H$_2$ = 96.5 bar, catalyst = 0.3 mM, T = 25 °C.

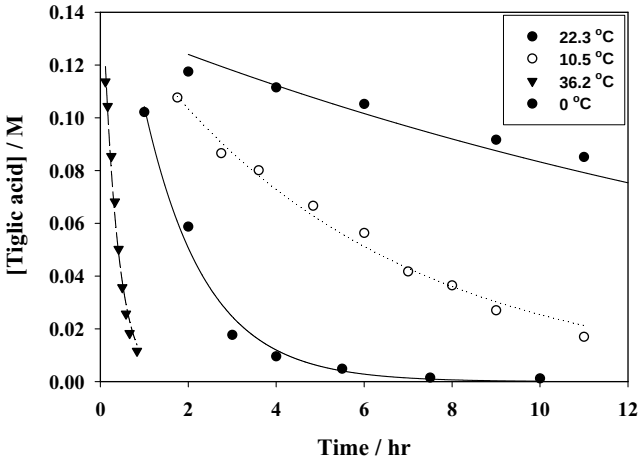

Fig. 7. Temperature effect on the tiglic acid hydrogenation reactions in methanol catalyzed by [(*p*-OCF_3)–BINAP]Ru[O_2CCH_3]$_2$ {H_2 = 95.3 bar, [catalyst] = 0.3 mM, [tiglic acid]$_0$ = 0.125 M}.

energies were 82.7 ± 1.9 kJ mol^{-1} and 80.1 ± 1.4 kJ mol^{-1} for reactions catalyzed by Ru–[(*p*-OCF_3)–BINAP] and Ru–BINAP, respectively. The former is slightly higher than the latter, which is also reflected in the difference in the rate constants, as shown in Section 2.6.

When Ru–[(*p*-OCF_3)–BINAP] was subjected to dense CO_2, it dissolved in CO_2 and the solution appeared homogeneous and had a yellowish color, in contrast with a colorless solution, and lots of solids stacked on the reactor surface when conventional Ru–BINAP complex was used. Further investigations showed that Ru–[(*p*-OCF_3)–BINAP] had sufficient solubility for catalysis in CO_2. Therefore, hydrogenation of tiglic acid with Ru–[(*p*-OCF_3)–BINAP] was also investigated in CO_2.

Preliminary experiments showed that the reactions proceeded smoothly in CO_2, but with a rather low enantioselectivity (around 25∼35%, which depended on the reaction temperature), in contrast with high enantioselectivity obtained in methanol. Therefore, methanol was added as a cosolvent or more properly, as a promoter, to the reaction system. Not surprisingly, the enantioselectivity jumped from 25 ∼ 35 to 50 ∼ 60%. Therefore, all of the reactions in CO_2 were carried out with added methanol (1 ml).

Table 2
Variation of enantioselectivity in CO_2

Conditions		ee (%)
$[H_2]_0$ (bar)[a]	0.7	57.3
	30	54.0
	50	55.1
[Tiglic acid]$_0$ (mM)[b]	37.0	51.6
	92.5	56.6
	185.5	62.5
[Catalyst] (mM)[c]	0.08	55.3
	0.24	56.6
	0.37	53.2

[a] [Tiglic acid]$_0$ = 92.5 mM, [catalyst] = 0.24 mM, *P* (total) = 166 bar, *T* = 25 °C, methanol = 1 ml.
[b] $[H_2]_0$ = 30 bar, [catalyst] = 0.24 mM, *P* (total) = 166 bar, *T* = 25 °C, methanol = 1 ml.
[c] $[H_2]_0$ = 50 bar, [tiglic acid] = 92.5 mM, *P* (total) = 166 bar, *T* = 25 °C, methanol = 1 ml.

Since hydrogen is miscible with CO_2, in order to compare the results with the results of hydrogen pressure effect on enantioselectivity in methanol at the same hydrogen concentration in the catalyst phase, the hydrogen pressures used for reactions in CO_2 were selected to range from 0.7 to 50 bar. Unlike in methanol, enantioselectivity was not affected by hydrogen pressure for reactions in CO_2, as shown in Table 2. This probably results from the fact that the surrounding environment for the reaction intermediates was CO_2 instead of methanol, which changed the ligand exchange step. We also investigated the hydrogen pressure effect on reaction rate. As shown in Fig. 9, it seems that

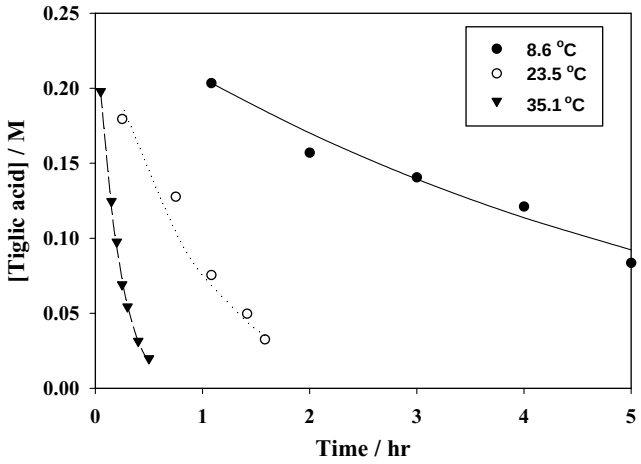

Fig. 8. Temperature effect on the tiglic acid hydrogenation reactions in methanol catalyzed by [BINAP]Ru[O_2CCH_3]$_2$ {H_2 = 95.3 bar, [catalyst] = 0.3 mM, [tiglic acid]$_0$ = 0.125 M}.

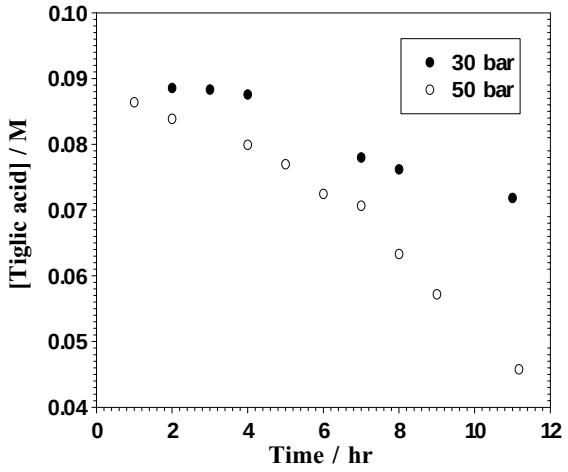

Fig. 9. Hydrogen pressure effect on the tiglic acid hydrogenation reactions in CO_2 by [(*p*-OCF_3)–BINAP]Ru[O_2CCH_3]$_2$ {[tiglic acid]$_0$ = 92.5 mM, [catalyst] = 0.24 mM, *P* (total) = 166 bar, methanol = 1 ml, *T* = 25 °C}.

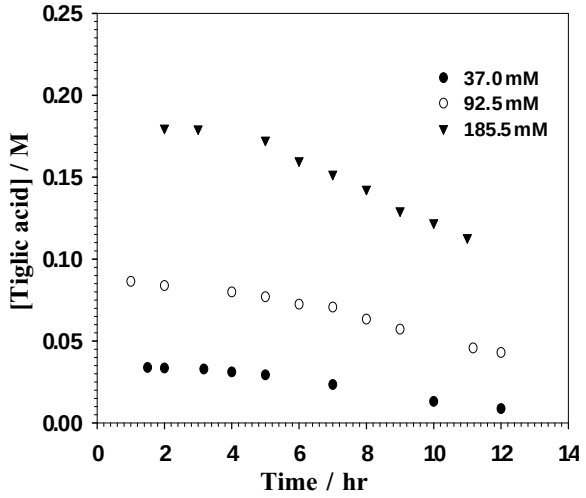

Fig. 10. Tiglic acid concentration effect on the tiglic acid hydrogenation reactions in CO_2 by [(*p*-OCF_3)–BINAP]Ru[O_2CCH_3]$_2$ {H_2 = 30 bar, [catalyst] = 0.24 mM, *P* (total) = 166 bar, methanol = 1 ml, *T* = 25 °C}.

high hydrogen pressures speeded up the formation of active species.

Substrate concentration effects in CO_2 were investigated by varying the initial tiglic acid concentration from 37.0 to 186.5 mM. The results, as shown in Fig. 10 and Table 2, indicate that the substrates with 2 carboxyl groups had a smaller effect on reactions in CO_2 than those in methanol. Interestingly, the substrate concentration was found to have a positive effect on enantioselectivity, which is shown in Table 2. The effect of catalyst concentration on reaction rate was also investigated by varying the catalyst concentration from 0.08 to 0.37 mM. As shown in Fig. 11, conversion was found to increase with increasing catalyst concentration, however the increase was not linear as would be expected.

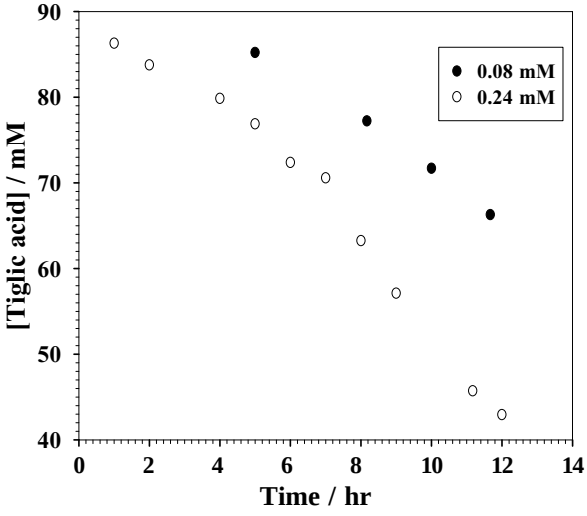

Fig. 11. Catalyst concentration effect on the tiglic acid hydrogenation reactions in CO_2 by [(*p*-OCF_3)–BINAP]Ru[O_2CCH_3]$_2${H_2 = 50 bar, [tiglic acid]$_0$ = 92.5 mM, *P* (total) = 166 bar, methanol = 1 ml, *T* = 25 °C}.

The enantioselectivity remained almost the same even the catalyst concentration was increased by a factor of three, which is shown in Table 2.

4. Discussion

It has been proposed that the tiglic acid hydrogenation by Ru–BINAP proceeds through a monohydride mechanism [16,18]. According to Ashby and Halpern [16], the reaction is first order in hydrogen at sufficiently low hydrogen pressures when the heterolytic split of hydrogen by the ruthenium–olefin complex is the rate determining step. At sufficiently high hydrogen pressures, hydrogen will trap every molecule of the complex and the reaction of ruthenium complex with olefin becomes the rate determining step and the reaction is zero order in hydrogen. At intermediate values of hydrogen pressure, the order will gradually change from 1.0 to 0.0. The order of 0.6 observed indicates that the experiments carried out in this study may fall into this intermediate region.

A mechanism which includes an additional hydride route to the olefin route proposed by Ashby and Halpern [16] is also a possibility and this mechanism is depicted in Fig. 12. These two routes were also proposed for the hydrogenation of vinylcarboxylic acid derivatives catalyzed by the conventional Ru–BINAP complex [19]. In this study, the hydride route was dominant at high hydrogen pressures and consisted of the following elementary steps:

1. the formation of a ruthenium monohydride intermediate,
2. the subsequent coordination of tiglic acid to the monohydride intermediate (which is the rate-determining step under a high hydrogen pressure),
3. hydride migration to the olefin,
4. oxidative addition of H_2 and reductive elimination of the product.

The olefin route, on the contrary, was dominant at low hydrogen pressures. In this case, the hydrogenation involved first coordination of tiglic acid to form the active complex by ligand exchange reactions where the carboxylate group was replaced by the tiglic acid. Subsequently, tiglic acid–Ru-hydride intermediate formed which is the rate-determining step under a low hydrogen pressure. Based on the references [16,18,20], the hydrogen migration step might be fast and the Ru–C bond can be cleaved by H_2 and/or methanol.

It is important to note that there was an induction period in the reactions in methanol catalyzed by Ru–[(*p*-OCF_3)–BINAP]. The induction period is usually an indication of expulsion of a ligand in order to provide a catalytically active site. The occurrence of an induction period indicates that the bond strength between the ruthenium and the carboxylate group increases with modification of the BINAP ligand, which is in agreement with the analysis of electronic properties of modified BINAP ligand and parent BINAP

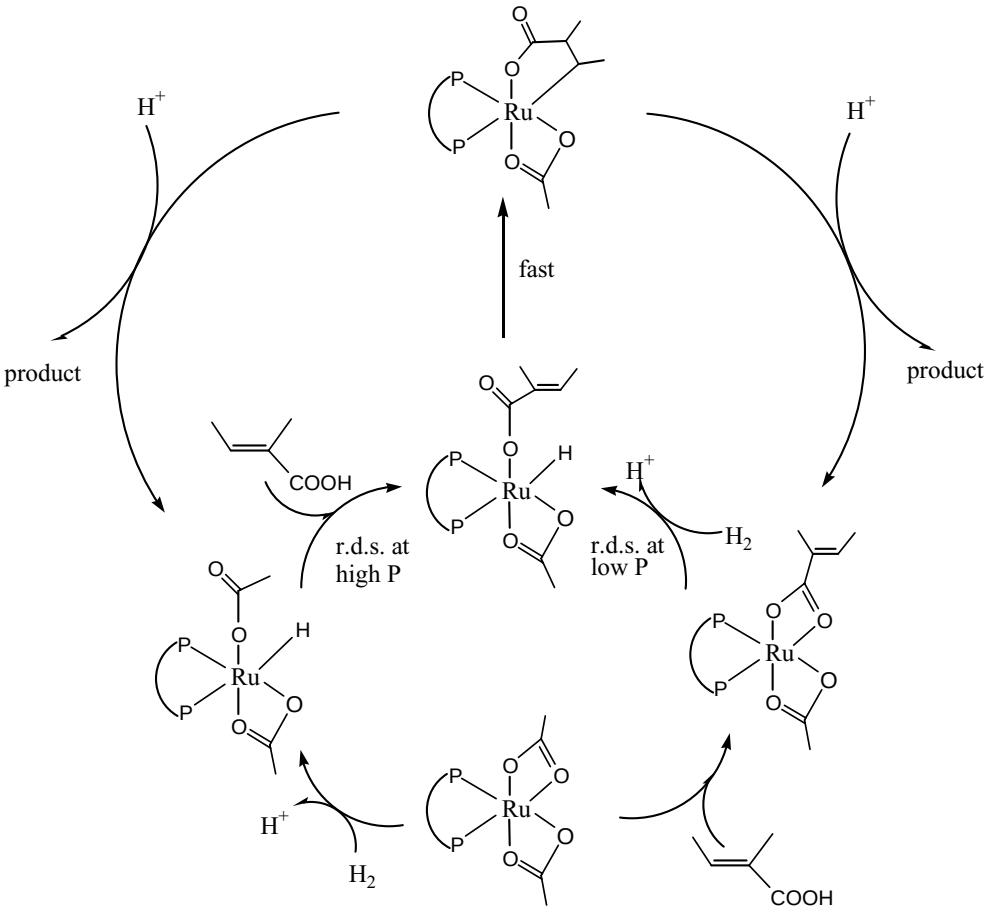

Fig. 12. Possible reaction pathway for hydrogenation of tiglic acid using ruthenium–BINAP complex.

ligand (^{31}P NMR and ^{1}H NMR spectra indicate that the OCF_3 groups withdraw the electrons from the phosphine). Thus, more time is needed to replace the carboxylate groups at the beginning of the reaction. Once reaction starts, the replaced carboxylate group will not participate in the catalytic cycle. This is in agreement with the proposed mechanism.

Though the effect of hydrogen pressure on enantioselectivity for Ru–BINAP is similar for Ru–[(*p*-OCF_3)–BINAP], a more detailed comparison between the two systems reveals some interesting differences. At low hydrogen pressures, the enantioselectivities obtained with both of the complexes were similar. However, for Ru–BINAP, the enantioselectivity dropped sharply (from 90 to 50%) when the hydrogen pressure increased from 3.4 to 95.3 bar, whereas the decrease in enantioselectivity (from 89 to 77%) was much less for Ru–[(*p*-OCF_3)–BINAP], as shown in Fig. 4. This probably results from the fact that Ru–[(*p*-OCF_3)–BINAP] complex might stabilize the monohydride species much better than Ru–BINAP complex due to a stronger ruthenium hydride bond. If one considers that the absolute configuration of the product is determined only by the step associated with the formation of five-membered ring of metal-alkyl intermediate, the stronger bond strength would provide more time for the coordinated tiglic acid to rearrange to the right position before the hydrogen migration to the olefin bond. As a result, the enantioselectivity with Ru–[(*p*-OCF_3)–BINAP] is higher than that with conventional Ru–BINAP at high hydrogen pressures.

The reaction in CO_2 might follow a different path. As stated in Section 3, with the addition of a small amount of methanol such as 1 ml, the increase in enantioselectivity was very sharp (from 30 to 56%). It was also noticed that the substrate concentration had no effect on enantioselectivity in methanol but had a positive effect in CO_2. The results can probably be attributed to the change of solvent properties. Increasing the acid or methanol concentration increases the polarity of the CO_2 and makes it more like a protic solvent. This helps with the dissociation of metal-alkyl intermediate bond and changes the equilibrium distribution of the enantiomer intermediates [18,20].

5. Conclusions

Fluorinated Ru–BINAP catalyst was developed with OCF_3-substitution of the aryl groups in BINAP skeleton. The properties of the catalyst in the tiglic acid hydrogenation reactions were investigated in the conventional solvent

methanol as well as in dense carbon dioxide. The effects of fluorous groups that were incorporated to the conventional BINAP on the catalysts were also investigated. The main conclusions are as follows:

1. The rate expressions for tiglic acid hydrogenation reactions in the presence of both the fluorinated catalyst and the conventional catalyst in methanol were derived. The orders for both hydrogen and tiglic acid were similar for both catalysts. The reaction rate constant with Ru–[(*p*-OCF_3)–BINAP] was lower than that with conventional catalyst due to the electron withdrawing property of incorporated OCF_3 groups.
2. A mechanism for reactions in methanol, which involves two routes, was proposed. The mechanism doesn't seem to change with modification of the catalyst. The similar orders obtained for hydrogen and tiglic acid for both catalysts seems to substantiate this.
3. At low hydrogen pressures, the enantioselectivity with Ru–[(*p*-OCF_3)–BINAP] was almost the same as that with Ru–BINAP. At higher hydrogen pressures, the enantioselectivity with Ru–[(*p*-OCF_3)–BINAP] complex was much higher.
4. The modified fluorinated catalyst had a much higher solubility in dense CO_2 than the conventional catalyst.
5. CO_2 had a great influence on both the activity and enantioselectivity.
6. Addition of methanol to CO_2 was found to increase the enantioselectivity.

Acknowledgements

The authors thank Dr. Martha Morton of University of Connecticut and Professor Richard L. Schowen and Professor Rich Given of the University of Kansas for very helpful discussions.

References

[1] S.C. Stinson, Chem. Eng. News 1 (2001) 79.
[2] P.G. Jessop, W. Leitner (Eds.), Chemical Synthesis Using Supercritical Fluids, 1999.
[3] J. Dupont, R.F. de Souza, P.A.Z. Suarez, Chem. Rev. 102 (2002) 3667.
[4] I.T. Horvath, J. Rabai, Science 266 (1994) 72.
[5] M.H. Abraham, A.H. Zissimos, J.G. Huddleston, H.D. Willauer, R.D. Rogers, W.E. Acree, Ind. Eng. Chem. Res. 42 (2003) 413.
[6] G. Pozzi, F. Cinato, Chem. Commun. 8 (1998) 877.
[7] Y. Nakamura, S. Takeuchi, K. Okumura, Y. Ohgo, D.P. Curran, Tetrahedron 58 (2002) 3963.
[8] M. Cavazzini, A. Manfredi, F. Montanari, S. Quici, G. Pozzi, Eur. J. Organic Chem. 24 (2001) 4639.
[9] S. Takeuchi, Y. Nakamura, Y. Ohgo, D.P. Curran, Tetrahedron Lett. 39 (1998) 8691.
[10] G. Francio, K. Wittmann, W. Leitner, J. Organomet. Chem. 621 (2001) 130.
[11] D.R. Palo, C. Erkey, Organometallics 19 (2000) 81.
[12] S. Fujita, S. Fujisawa, B.M. Bhanage, Y. Ikushima, M. Arai, New J. Chem. 26 (2002) 1479.
[13] S. Haji, C. Erkey, Tetrahedron 58 (2002) 3929.
[14] J.J. Juliette, I.T. Horvath, J.A. Gladysz, J. Am. Chem. Soc. 121 (1999) 2696.
[15] S. Akutagawa, Appl. Catal. A 128 (1995) 171.
[16] M.T. Ashby, J. Halpern, J. Am. Chem. Soc. 113 (1991) 589.
[17] K. Radhakrishnan, P.A. Ramachandran, P.H. Brahme, R.V. Chaudhari, J. Chem. Eng. Data 28 (1983) 1.
[18] T. Ohta, H. Takaya, R. Noyori, Tetrahedron Lett. 31 (1990) 7189.
[19] A.S.C. Chan, C.C. Chen, T.K. Yang, J.H. Huang, Y.C. Lin, Inorg. Chim. Acta 234 (1995) 95.
[20] M. Kitamura, M. Tsukamoto, Y. Bessho, M. Yoshimura, U. Kobs, M. Widhalm, R. Noyori, J. Am. Chem. Soc. 124 (2002) 6649.